
ADAPTIVE NANOPORE SEQUENCING ON MINIATURE FLOW CELL DETECTS EXTENSIVE ANTIMICROBIAL RESISTANCE

PREPRINT

1 Adrian Viehweger ^{1*}, Mike Marquet ², Martin Hölzer ³, Nadine Dietze ¹, Mathias W. Pletz ², Christian Brandt ²

2 ¹ Institute of Medical Microbiology and Virology, University Hospital Leipzig, Leipzig, Germany ² Institute for
3 Infectious Diseases and Infection Control, Jena University Hospital, Jena, Germany ³ Methodology and Research
4 Infrastructure, MF1 Bioinformatics, Robert Koch Institute, Berlin, Germany

5 * Corresponding author: adrian.viehweger@medizin.uni-leipzig.de

6 **Abstract**

7 Rapid screening of hospital admissions to detect asymptomatic carriers of resistant bacteria can prevent pathogen
8 outbreaks. However, the resulting isolates rarely have their genome sequenced due to cost constraints and long turn-
9 around times to get and process the data, limiting their usefulness to the practitioner. Here we use real-time, on-device
10 target enrichment ("adaptive") sequencing on a new type of low-cost nanopore flow cell as a highly multiplexed assay
11 covering 1,147 antimicrobial resistance genes. Using this method, we detected three types of carbapenemase in a
12 single isolate of *Raoultella ornithinolytica* (*NDM*, *KPC*, *VIM*). Further investigation revealed extensive horizontal gene
13 transfer within the underlying microbial consortium, increasing the risk of resistance spreading. From a technical point
14 of view, we identify two important variables that can increase the enrichment of target genes: higher nucleotide identity
15 and shorter read length. Real-time sequencing could thus quickly inform how to monitor this case and its surroundings.

16 **Keywords** Nanopore sequencing · Target enrichment · Antimicrobial Resistance · Carbapenemases · Plasmids

17 **Background**

18 Screening patients for multiresistant bacteria on hospital admission can detect asymptomatic colonization early ^[1] and
19 reduce subsequent complications. ^[2] However, corresponding isolates rarely have their genome sequenced, which would
20 enable genomic surveillance, and, as a result, source control and reduced spread. ^[3] Such resistant strains can colonize
21 patients for years, increasing the value of this information. ^[4] Long-term carriage is surprising in the absence of a
22 selective stimuli such as treatment with antimicrobials. Recently, the underlying microbial consortia in which these
23 strains are embedded have been implicated in resistance maintenance through ongoing horizontal gene transfer of
24 mobile elements. ^{[5][6]} This finding suggests that in special cases, genomic surveillance should be expanded to include
25 metagenomic data. ^[7]

26 Here we report on a patient with multiple carbapenem-resistant strains detected in a rectal swab. One of the isolates
27 simultaneously carried four carbapenemases, an unusually high number. To support a timely response, we integrated the
28 results from multiple modalities of real-time nanopore sequencing. First, we reconstructed the genomes of individual
29 isolates and then complemented them with metagenomic data from the swab. In a proof-of-concept, we then applied
30 real-time on-device target enrichment of 1,147 resistance genes on a miniature flow cell⁸ to create an ultra-high multiplex
31 assay.

32 Results

33 During resistance screening of rectal swabs, we found three bacterial species growing on carbapenem agar (*Raoultella*
34 *ornithinolytica*, *Citrobacter freundii*, and *Citrobacter amalonaticus*). The patient's history revealed no apparent source,
35 although past occupations included work in waste management and training in agriculture, both of which have increased
36 exposure to antibiotic resistance genes.⁹ Surprisingly, we detected multiple carbapenemases in *R. ornithinolytica* using
37 PCR (*NDM*, *KPC*, *VIM*). To identify all resistance genes in the isolates and any putative horizontal transfer between
38 them, we performed real-time nanopore sequencing, both of the isolates individually and of the entire rectal swab,
39 generating in total 3.9 M reads and 23.3 Gb on a standard ("MinION") flow cell.

40 The *R. ornithinolytica* isolate carried nine plasmids and three carbapenemases: *NDM-1*, *KPC-2*, and *VIM-1* (Figure **I**A).
41 All carbapenemases were encoded on one plasmid each, except *VIM*, which was located on the bacterial chromosome.

42 The two *Citrobacter* isolates only carried *VIM-1*. An alignment of the genomic region 10 Kb upstream and downstream
43 of *VIM* across the isolates revealed a transposase-mediated resistance transfer, for which we propose the following
44 gene flow: The genomes of *C. freundii* and *C. amalonaticus* both carry *VIM-1* on an *IncHI2* plasmid (> 95 %
45 sequence identity). In *C. freundii*, this transposon then likely copied itself into an *IncN* plasmid with the help of an
46 *ISKpn19* transposase (Figure **I**B). The same transposase is found flanking the *VIM* transposon in the *R. ornithinolytica*
47 chromosome, which makes the *IncN* plasmid of *C. freundii* its likely source. A similar transfer pattern was observed for
48 the penicillinase *OXA-1* (data not shown).

49 Isolate sequencing captured 79.7 % of resistance genes detected in the underlying microbial consortium through
50 metagenomic sequencing (total yield 10 Gb, Figure **I**C). Of the remainder, few genes were clinically relevant, such as
51 several efflux pumps. Other resistance genes were associated with Gram-positive bacteria, which we did not screen for
52 with culture (Figure **I**C). Surprisingly, metagenomics did not detect five resistance gene types (6.8 %), including *KPC*,
53 two out of three *OXA* copies, and two out of four *VIM* copies. This omission likely occurs because the metagenome was
54 dominated by *Proteus vulgaris* (44.6 % of reads), leaving fewer reads (depth) for the carbapenemase-carrying strains
55 (*C. freundii* 19.7 %, *R. ornithinolytica* 1.8 %, *C. amalonaticus* 0.01 %). Selective culture enriched these low-abundant
56 species.

57 We also observed substantial horizontal gene transfer between our isolate members of the *Enterobacteriaceae* (Fig-
58 ure **I**D). For example, *C. freundii* and *R. ornithinolytica* share 15 loci. A region was labeled as a putative transfer
59 if its length exceeded one kilobase with 99.9 % sequence identity between any two genomes. No additional transfer
60 was found in two uncultured, metagenome-assembled genomes (MAGs), namely *Enterococcus faecium* and *Serratia*

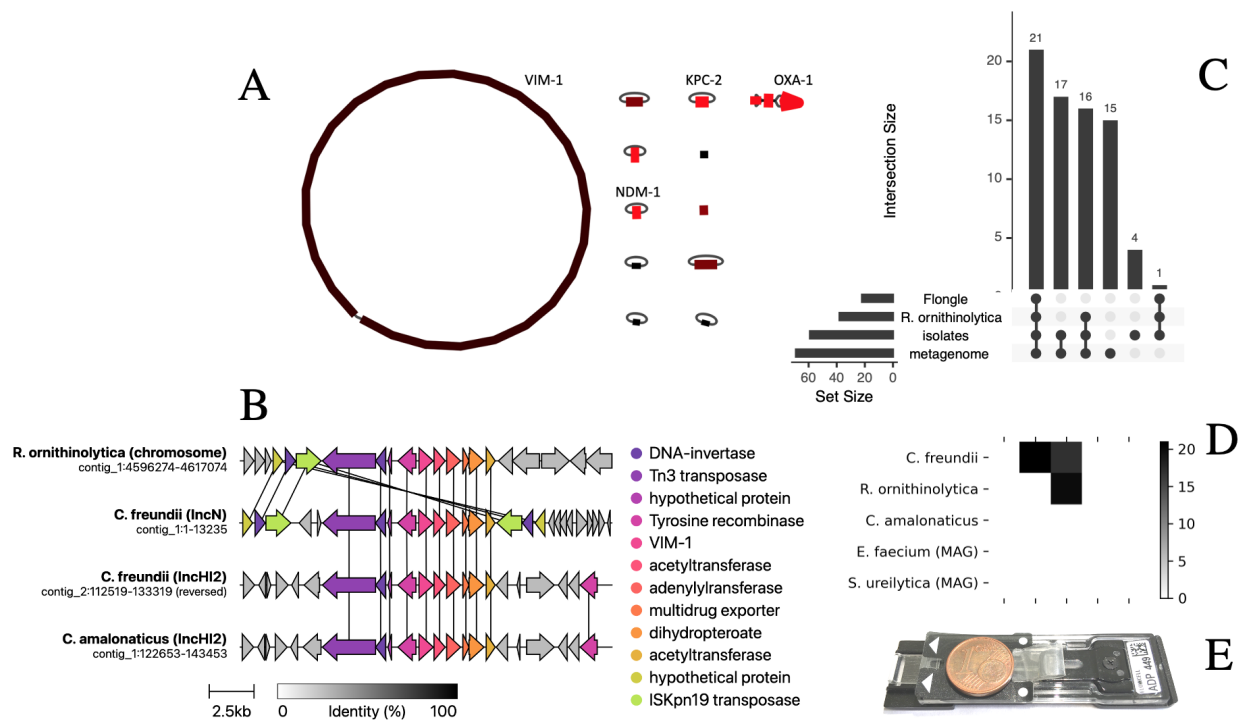


Figure 1: Real-time sequencing reveals extensive resistance load and horizontal gene transfer. **(A)** Genome reconstruction of a strain of *R. ornithinolytica* carrying nine plasmids and four carbapenemase genes. Color-coded coverage from 90x (black, e.g., chromosome) to 250x (red, e.g., plasmid carrying *OXA-1*). **(B)** Gene transfer of *VIM-1* across three strains and four loci. The carbapenemase is flanked by multiple transposases (see annotation), which likely mediate its mobilization. Vertical lines indicate 100% sequence identity between corresponding genes. **(C)** Comparison of shared resistance genes between the enrichment sequencing run ("Flongle"), the *R. ornithinolytica* isolate, all four "isolates" combined and the "metagenome" assembly. Of all resistance genes identified in the metagenome, 79.7% were found in the isolates. Surprisingly, several resistance genes were not identified in the metagenome, among them several carbapenemase copies. In the *R. ornithinolytica* isolate genome, about two-thirds of resistance genes were also found using on-device target enrichment. All plasmid-encoded genes among them were detected, including all carbapenemases. **(D)** Pairwise shared sequences between isolates and metagenome-assembled genomes. Putative transfers were defined as loci with a minimum length of one kilobase and 99.9% sequence identity between each pair of loci. Extensive sequence transfer is observed between the three isolate genomes (and their corresponding bins from the metagenomic assembly). **(E)** Miniature, low-cost flow cell used for on-device target enrichment ("Flongle", Oxford Nanopore Technologies), with a one-cent coin placed on top as scale.

61 *ureilytica*. None of the remaining metagenomic contigs showed putative transfers. Again, metagenomics did not add
62 important information beyond the culture isolates.

63 The sensitivity of metagenomic sequencing can be increased with depth, but the associated cost limits the applicability
64 in the routine laboratory. Therefore, going in the opposite direction, a recently introduced miniature nanopore flow cell
65 ("Flongle") aims to reduce per-run costs through reduced sequencing yield. Because the yield is reduced, however,
66 targeted sequencing of relevant genes or loci is desirable. Such target enrichment can be performed "on-device", i.e.,
67 during the sequencing run in real-time and without any changes in the sample preparation, using a method also known
68 as nanopore "adaptive sequencing"^[10,12]. Here, reads are rejected from the pore when the read fragment that already
69 passed through it does not match any sequence in a target database. The nanopore is then free to sequence another
70 molecule.

71 Adaptive sequencing can be used to enrich or deplete either entire organisms from a sample of DNA or to target specific
72 genes.^{[1][2]} Here we aimed to enrich 1,147 representative antimicrobial resistance genes (ARGs, see methods), which to
73 our knowledge, is the first time that adaptive sequencing has been used to target a microbial gene panel. We define
74 "enrichment" as the difference in total read count over a corresponding ARG between standard and adaptive sequencing.
75 In the latter condition and unless stated otherwise, we exclude rejected reads, i.e., those for which the adaptive selection
76 algorithm has not recognized a target in the first bases of the read (Figure [S1](#)).

77 Read count over target genes is a commonly used metric in RNA-Seq experiments, with two caveats: First, most
78 RNA-Seq studies use fixed-sized short reads, i.e., the read length distribution is the same for all conditions. Second, the
79 read count is normalized by target length and the overall number of mapped reads, which allows the comparison of
80 targets *within* a condition ("relative expression"), although their size might differ. Here, we only use raw read count
81 to measure enrichment without further adjustments. We justify this because, first, a single library was used in both
82 conditions (standard, adaptive), and the resulting read length distributions for "standard" and "unrejected adaptive"
83 reads are near-identical (Figure [S1](#)). Second, we only compare each target *across* conditions, and so there is no need to
84 normalize by target length.

85 To compare target read abundance between adaptive and "standard" nanopore sequencing, we sequenced three isolates
86 in technical duplicates on a single MinION flow cell, periodically alternating between adaptive and standard sequencing
87 in 16 one-hour intervals (Figure [2A](#)). Overall, adaptive sequencing could roughly double the abundance of many targets,
88 while others were hardly detected at all (Figure [2B](#)). We subsequently identified two factors that substantially affected
89 target abundance between the two conditions: nucleotide identity and read length.

90 First, high nucleotide identity between an isolate's gene and the corresponding member of the target gene panel resulted
91 in a higher on-target read count (Figure [2B](#)). Surprisingly, most similar and thus most enriched genes were located on
92 plasmids. This likely reflects a bias in the database composition, where common resistance plasmids are well annotated
93 while strain-specific, chromosomal gene isoforms are undersampled. As expected, target sequence similarity did not
94 affect abundance in the standard condition, which did not use a target database. To quantify this effect, we performed
95 Bayesian regression and modeled the effects of variables for which a contribution to abundance seemed plausible,
96 namely sequence similarity, coverage, read length and whether the target was located on a plasmid (including interaction
97 effects, see methods). The largest effect was observed for similarity conditional on whether adaptive sequencing was
98 turned on ($\beta = 11.98$, 95 % $CI \pm 0.15$). However, it can be hard to interpret any single coefficient in an interaction
99 model in isolation; it is more informative to plot samples from the posterior distribution for any variable of interest. All
100 else being equal, adaptive enrichment only outperforms standard sequencing when an isolate's gene has a nucleotide
101 identity of at least 95 % to a record in the target database, and up to two-fold for near-identical targets (Figure [2C](#)).
102 Several targets are enriched four times over the standard baseline. Other studies reported a similar enrichment of two-
103 to four-fold for bacterial genomes, albeit partly using different real-time matching algorithms.^{[1][13]}

104 Second, we observed that reads from plasmids were shorter than chromosomal ones (Figure [2D](#)). Furthermore, the
105 length of chromosomal reads is shorter for adaptive sequencing than the standard because if a target is not identified on
106 a given read, sequencing is terminated prematurely. Our statistical model takes this conditionality into account. The
107 model indicates that adaptive sequencing outperforms the standard only for reads smaller than 3 kb, all else being equal

108 (Figure 2E). This bias contributes to the higher target abundance for plasmid-encoded genes than chromosomal ones
109 within the adaptive sequencing condition.

110 It seems counterintuitive that short reads are enriched more than longer ones. However, this is due to how adaptive
111 sequencing rejects reads. The algorithm scans the first part of each read for target sequences, and if none is found
112 after several hundred bases, the read is rejected (median 415 bases, Figure S1). To further investigate the relationship
113 between read length, target length, and false-negative rate (FNR), we simulated combinations of, e.g., long reads and
114 short targets and short reads and long targets (see methods). A fixed-length target occupies a smaller fraction in long
115 reads than in shorter ones. We find that the smaller this fraction, the higher the false-negative rate, i.e., the more reads
116 which contain the target are falsely rejected (Figure S3). The intuition behind this result is that a target has many
117 potential starting points on a read. The longer the read and the shorter the target, the more likely the target starts at a
118 position after the read interval that the selection algorithm uses for its decision.

119 The relative abundance of reads *outside of target regions* should not change during adaptive sequencing.¹² We checked
120 this by comparing the coverage of "standard" and "rejected adaptive" reads across assembly contigs, which did not
121 differ substantially (Figure S2). Note that we normalize coverage to that of the chromosome for both read sets because
122 the rejected reads from the adaptive condition are much shorter and more numerous (Figure S1, median read length
123 3,194 vs. 415 bases).

124 We then tested the enrichment on a new type of miniature, low-cost flow cell and generated 5.4 Mb within four hours
125 from the carbapenemase-rich *R. ornithinolytica* isolate (Figure 1E). 97.2% of reads were rejected; of those, 0.2%
126 (n=43) were false negative. Correspondingly, 2.8% of reads were accepted, of which 20.4% (n=104) were true positive,
127 i.e., could be found in the target database. A positive database hit was defined as a read with at least 100 bp mapped to a
128 target with a minimum of 50% matching positions. 57.9% of the resistance genes found in the high-quality genome
129 reconstruction were found using adaptive sampling, too, including all four carbapenemases (Figure 1C). As expected
130 from the adaptive-standard state switching experiment, the probability of detection was determined by genomic location:
131 All un-detected genes were located on the chromosome, and all plasmid-encoded resistance genes were detected (odds
132 ratio 26.7, $p < 0.001$). While plasmids are present in higher copy numbers relative to the chromosome (Figure 1A),
133 our regression model did not assign a large effect to this variable. Since many resistance determinants are located on
134 plasmids, we argue that enrichment sequencing is a promising approach for antimicrobial gene detection in routine
135 settings.

136 Discussion

137 We detected a highly resistant consortium during hospital admission screening, including a strain that carried three
138 carbapenemases. Nanopore sequencing comprehensively characterized three resistant culture isolates, documenting
139 many resistance genes as well as extensive gene transfer between isolates. Metagenomic sequencing of the corresponding
140 rectal swap added little information and did not detect several important resistance genes. It might be that deeper
141 sequencing would increase sensitivity. Still, because the carbapenemase-carrying strains were low abundant, in practice,
142 this procedure would not be cost-competitive in a routine setting. Cultural screening as a first step reliably identified the
143 strains that carried clinically relevant resistance genes within 24 hours from sample streaking on screening agar plates to
144 detectable growth. From subsequent sequencing, including library preparation to isolate genome assembly, another 24

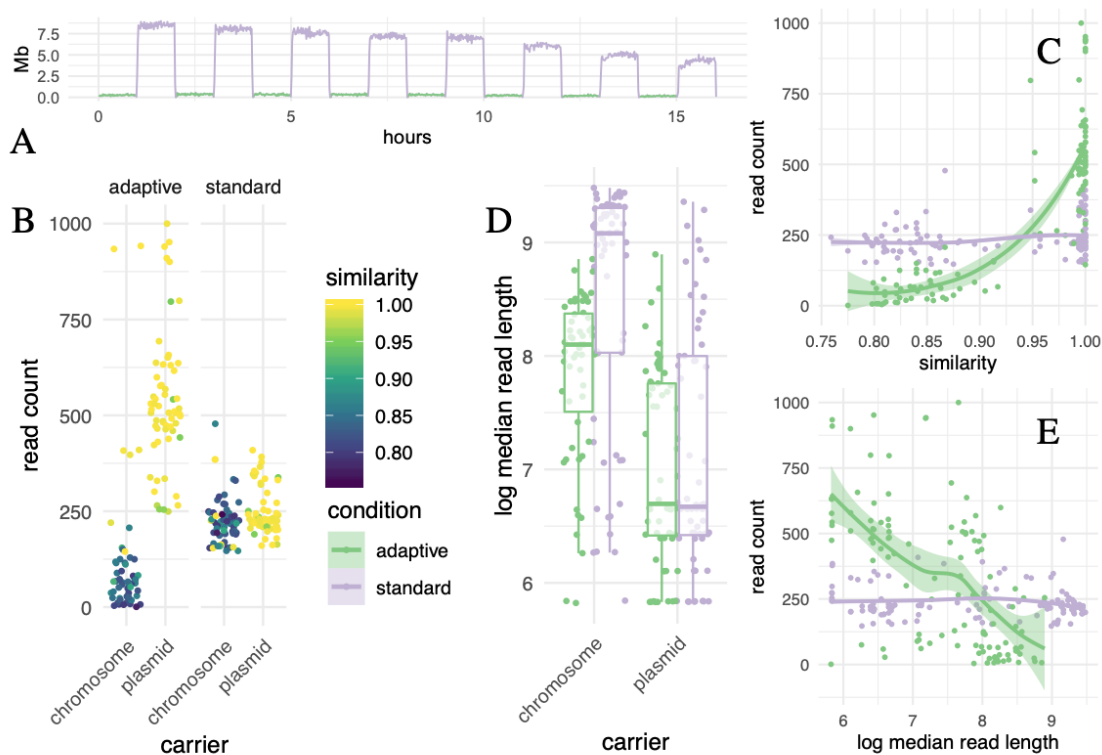


Figure 2: Effect of two variables during *adaptive* sequencing on enrichment efficiency compared to a *standard* nanopore sequencing run. **(A)** The same three *Citrobacter* and *Raoultella* isolates were sequenced with and without enrichment (green and violet, respectively), alternating the conditions periodically on a single flow cell. **(B)** Each point corresponds to an open reading frame that has been annotated in the final isolate genome assembly as a resistance gene using a dereplicated ARG database (n=1,147). "Read count" is the number of reads from each sequencing condition that map to these genes. As the read passes through the nanopore during enrichment, it is searched in real-time against a database of target genes. If no match is found, the read is ejected prematurely. Reads that are very *similar* to a database entry (nucleotide identity) pass this filter, while reads with lower sequence identity are falsely rejected. Many highly similar targets reside on plasmids, likely a sampling bias in the resistance database. As expected, similarity has no effect on read count per ORF for standard sequencing because there is no database search involved. **(C)** Adaptive sequencing outperforms the standard once the nucleotide identity ("similarity") between the target and its match in the panel database surpasses 95 %. For values close to identity, a two-fold enrichment can be expected. We even observed a four-fold enrichment of several targets over the standard baseline. When we fit a Bayesian multivariate regression model, the increase of target abundance with similarity becomes clear (2.5 and 97.5 % quantiles displayed). **(D)** Reads derived from plasmids are shorter than chromosomal ones. In turn, chromosomal reads from adaptive are shorter than those from standard sequencing because they are more frequently ejected from the nanopore before the read has been sequenced fully for lack of any match. These factors need to be accounted for in a regression model to estimate the effect of read length on target abundance accurately. **(E)** Adaptive sequencing outperforms the standard for shorter read lengths of 3 kb and less, all else being equal. Short reads of about 1 kb can potentially double target abundance. Therefore, library preparation protocols for adaptive sequencing could add a step to shear extracted DNA to improve the enrichment.

145 hours passed. This short turn-around time helped shape the public health response. For example, transposon-encoded
 146 *VIM* and *OXA* meant that associated wards could be monitored for the occurrence of these genes in other members of
 147 the *Enterobacteriaceae*. By comparison, generating 20 Gb of metagenomic data would also take two days, irrespective

148 of the sequencing platform. In addition, more computation is required for the final assembly, binning, and validation of
149 the mixed sample.

150 We then evaluated a new approach for on-device, real-time target enrichment called "adaptive sequencing". It en-
151 compassed 1,147 representative antimicrobial resistance genes in an ultra-high multiplex assay. In the enrichment
152 sequencing data, reads were detected for all resistance genes known to be present in the isolate assemblies from
153 an independent, previous sequencing run (see methods). However, while some genes could be enriched up to four
154 times over the baseline, others were hardly captured. To explain the disparity, we found that two variables influence
155 enrichment substantially. First, the higher the nucleotide similarity of a read to its corresponding entry in the target
156 database, the more reads were selected. Adaptive outperformed standard sequencing above 95 % identity. Optimization
157 of the target database to reflect the expected targets as closely as possible is thus crucial. Future studies will have to
158 determine the influence of database size and redundancy on target abundance. Second, we showed that fragments shorter
159 than 3 kb are beneficial to target abundance. Counterintuitively for nanopore sequencing, deliberate shearing of DNA
160 fragments during library preparation should help to enrich targets. From an economics perspective, the fold-enrichment
161 is inversely proportional to sequencing cost. So an enrichment by a factor of two would translate into 50 % reduced
162 sequencing costs (excluding library preparation).

163 The degree to which DNA should be sheared for an enrichment experiment depends on the underlying choice of target
164 length. For the enrichment of antimicrobial resistance genes, as demonstrated in this study and with a mean length of
165 about one kilobase, we recommend matching this with an equal median read length.

166 We then performed on-device target enrichment of the most resistant culture isolate on a new type of miniature flow cell
167 and were able to identify all plasmid-encoded resistance genes and nearly two-thirds of all resistance genes known to be
168 present.

169 **Conclusions**

170 As a proof of concept, we show that on-device target enrichment on low-cost flow cells could be a valuable complement
171 to routine microbiology. It takes us closer to an effective point-of-care resistance screening, especially given the
172 continued rapid improvements in the underlying technology.^[24] However, given the variable sequencing yield of this new
173 flow cell type, further controlled experiments that compare multiple runs with and without enrichment are warranted, as
174 are studies that optimize sample preparation and target database composition.

175 **Methods**

176 **Culture and DNA extraction**

177 All samples were streaked on carbapenemase chromogenic agar plates (CHROMagar, Paris, France). Carbapenemase
178 carriage was confirmed using PCR and phenotypically using microdilution MIC testing. DNA was extracted from
179 culture isolates and rectal swabs using the ZymoBIOMICS DNA Miniprep extraction kit according to the manufacturer's
180 instructions. The cell disruption was conducted three times for five minutes with the Speedmill Plus (Analytik Jena,
181 Germany).

182 **Library preparation**

183 DNA quantification steps were performed using the dsDNA HS assay for Qubit (Invitrogen, US). DNA was size-selected
184 by cleaning up with 0.45x volume of Ampure XP buffer (Beckman Coulter, Brea, CA, USA) and eluted in 60 l EB
185 buffer (Qiagen, Hilden, Germany). The libraries were prepared from 1.5 g input DNA. For multiple samples we
186 used the SQK-LSK109 kit (Oxford Nanopore Technologies, Oxford, UK) and the Native Barcoding Expansion-Kit
187 (EXP-NBD104), according to the manufacturer's protocol. For the Flongle run we used the SQK-RBK004 kit from the
188 same manufacturer.

189 **Nanopore sequencing and on-device target enrichment**

190 All DNA was sequenced on the GridION using a FLO-MIN106D (MinION) and FLO-FGL001 (Flongle) flow cells
191 (MinKNOW software v4.1.2), all from Oxford Nanopore Technologies. Three sequencing runs were performed: For the
192 first run (MinION flow cell) we multiplexed three culture isolates (A2, B1, B2) and a metagenomic sample (3.9 M
193 reads and 23.3 Gb in 48 h, about 10 Gb were metagenomic). The second run (MinION flow cell) was an experiment
194 comparing "adaptive" and "standard" sequencing. On a single flow cell, we periodically alternated between both states
195 by manually turning the sequencing run off and then back on in the other state in one-hour intervals for a total of 16
196 hours. Toggling between states did not harm sequencing (e.g., through pore blockages; 3.44 M reads and 4.47 Gb
197 in 16 hours). The sequencing yield for all barcodes from three isolates (two *Citrobacter* and one *Raoultella*) with
198 two technical replicates each was about equal. Adaptive sequencing groups the sequence data into "rejected", i.e.,
199 reads that do not contain a target, and "unrejected". The latter comprises reads with a target found and reads with a
200 pending decision. We used the unrejected reads pooled across isolates and replicates for all further analyses unless
201 stated otherwise. Pooled and per-isolate results did not differ substantially (compare Figure [2B](#) and [S4](#)). In the third
202 sequencing run (Flongle flow cell), only isolate A2 was included, and adaptive sampling was applied throughout (18,646
203 reads and 5.36 Mb in 4h).

204 As target database, we created a dereplicated version of the *CARD* database of resistance genes (v3.1.3)^[15] using
205 `mmseqs2 easy-cluster` (v13.45111)^[16] using a minimum sequence identity of 0.95 and minimum coverage of 0.8 in
206 coverage mode 1. We thereby reduced the database from 2,979 to 1,147 representative genes. We performed this step
207 to reduce the search space that the adaptive sequencing algorithm has to map against. The total length of all genes in
208 the database was 1.16 Mb. The reduction halves the database size because many resistance genes such as *CTX* have
209 many documented isoforms, which would lead to uninformative multi-mappings. Reads were basecalled using the
210 guppy GPU basecaller (high accuracy model, v4.2.2, Oxford Nanopore Technologies). For isolate genomes, reads
211 were assigned to their respective barcodes only if matching adapters were detected on both ends of the read to avoid
212 cross-contamination.

213 For the experiment comparing "adaptive" and "standard" sequencing on a single flow cell, we periodically alternated
214 between both states by manually turning the sequencing run off and then back on in the other state in one-hour intervals
215 for a total of 16 hours. This protocol did not have a negative effect on total sequencing yield over time (e.g., through
216 pore blockages). The sequencing yield for all barcodes from three isolates (two *Citrobacter* and one *Raoultella*) with
217 two technical replicates each was about equal. Adaptive sequencing groups the sequence data into "rejected", i.e., reads

218 that do not contain a target, and "unrejected". The latter comprises reads where a target has been found and reads with a
219 pending decision. We used the unrejected read fraction for all further analyses.

220 Data analysis

221 Isolate data were assembled using `flye` (v2.9)^[17] and consensus sequences corrected using three rounds of polishing
222 with `racon` (v1.4.3)^[18] followed by `medaka` (v1.4.3, unpublished, github.com/nanoporetech/medaka). Read mapping
223 was performed using `minimap2` (v2.22-r1101).^[19] Genome quality was confirmed using `checkm` (v1.1.3).^[20] All isolate
224 genome assemblies were > 99 % complete and < 1 % "contaminated" (duplicate single-copy marker genes), which
225 counts as high quality by community standards. Resistance gene annotation was performed using `abricate` (v1.0.1,
226 unpublished, github.com/tseemann/abricate) against the *CARD* database (see above). Taxonomic assignments were
227 performed using single-copy marker genes^[21] as well as k-mers using `sourmash` (v4.2).^[22]

228 For the long read-only metagenomic assembly we used `flye` with the `--meta` flag. We then mapped all reads to the
229 assembly using `minimap2`. We then used `racon` to perform three rounds of long read-only polishing of the assembly
230 using the alignment. Last, we used `medaka` to generate the final consensus assembly. Binning and annotation were
231 then performed as described elsewhere,^[23] by feeding the consensus assembly into the corresponding workflow modules
232 using default settings. Pairwise similarity between genes was calculated using `mmseqs2 easy-search` (v13.45111).^[16]
233 The amount of putative horizontal gene transfer between isolate genomes and MAGs was estimated by counting the
234 number of shared genes for each pair. First, we performed pairwise genome alignment using the `nucmer` command
235 from `mummer` (v4.0.0rc1).^[24] We then searched for "shared genes", defined as such if the alignment was 1 kb or longer
236 and if the pairwise nucleotide identity between genes was > 99.9 %.

237 To model the influence of several predictor variables on our outcome variable "target abundance" (total on-target read
238 count), including plausible interactions, we fit a Bayesian regression model using `brms` (v2.13).^[25] The outcome variable
239 was modeled as a Poisson distribution. We conditioned the effect of nucleotide similarity on sequencing state, i.e.,
240 whether adaptive sequencing was turned on or off, by introducing an interaction term. Also, we conditioned read length
241 on sequencing state and whether a read was derived from a plasmid or the chromosome. Finally, we included a term to
242 model the effect of contig coverage, calculated from mapping the reads back to the isolate assemblies.

$$\begin{aligned} read_count &\sim Normal(\mu_i, \sigma) \\ \mu_i &= \alpha + \gamma_i adaptive_i + \delta_i plasmid_i + \delta_i adaptive_i + \beta_1 coverage \\ \gamma_i &= \beta_2 + \beta_3 similarity \\ \delta_i &= \beta_4 + \beta_5 \log(read_length) \end{aligned}$$

243 Sampling was performed with four chains, each with 2,000 iterations, of which the first half were discarded as warmup,
244 for a total of 4,000 post-warmup samples. Samples were drawn using the NUTS algorithm. All chains converged
245 ($\hat{R} = 1.00$). Coefficient estimates including confidence intervals are available in Table S1. Refer to the project
246 repository for code on how the model was specified.

247 For the simulation experiment, we first determined that a log-normal distribution can adequately model the different
248 length distributions (Figure [S1](#)). We then selected parameters to model combinations of reads and targets of varying
249 length distributions, from long (mean 8,103 bases, or log 9, variance 1.5) to short (mean 665 bases, or log 6.5, variance
250 0.25). We could thus, for example, assess the effects of combining long reads with short targets and short reads with long
251 targets. Next, we generated ten thousand (read, target) sample pairs for each combination of read and target distributions.
252 For each pair, we randomly "placed" a target start on the read with a uniform distribution across read positions, in line
253 with how targets are distributed across DNA fragments in realistic single-molecule sequencing experiments. We then
254 asked if the first part of the read (as seen by the adaptive sampling algorithm) would have detected the target. Since all
255 simulated reads contain a target, failure to detect one in the first number of bases counts as a false negative (Figure [S3](#)).
256 To estimate effect sizes on the false-negative rate (FNR) we fit a multivariate regression model using brms (see above)
257 (Figure [S3](#)):

$$FNR \sim Normal(\mu_i, \sigma)$$
$$\mu_i = \alpha + \beta_1 \log(read_length) + \beta_2 \log(target_length)$$

258 **List of abbreviations**

259 ARG .. antimicrobial resistance gene, ORF .. open reading frame, MAG .. metagenome-assembled genome, FNR ..
260 false negative rate

261 **Ethics approval and consent to participate**

262 Not applicable; only microbial samples were used, which are not subject to ethical approval. Human DNA sequences
263 were removed from the metagenomic stool dataset before analysis by filtering them against the recently published
264 complete human reference genome "CHM13"²⁶

265 **Consent for publication**

266 Not applicable. The manuscript includes no specific details, images or videos relating to an individual person.

267 **Availability of data and materials**

268 All basecalled nanopore sequencing data has been deposited with the SRA, NCBI. Metagenomic reads are available
269 under project ID PRJNA788147. Reads from isolate genomes, the Flongle flow cell and the experiment alternating
270 between adaptive and standard state have been deposited under project ID PRJNA788148 under their respective sample
271 ID (*Raoultella ornithinolytica*: SAMN23928631, *Citrobacter freundii*: SAMN23928632, *Citrobacter amalonaticus*:
272 SAMN23928633).

273 Beyond standard analyses described in the methods, code and referenced assemblies (isolates, metagenome) for the
274 following analyses are available from a dedicated code repository at github.com/phiweger/adaptive; Putative horizontal

275 gene transfer, creation of the target database for adaptive sequencing, analysis of the experiment that switched adaptive
276 sequencing on and off and how to specify a Bayesian regression model of the target count.

277 **Competing interests**

278 AV has received travel expenses to speak at Oxford Nanopore meetings. AV, CB and MH are co-founders of nanozoo
279 GmbH and hold shares in the company.

280 **Funding**

281 None received.

282 **Authors' contributions**

283 AV designed the study. AV and ND collected and characterized all samples. MM and CB extracted DNA, prepared
284 Nanopore libraries, and performed all sequencing experiments. AV, CB, and MH analyzed the data. All authors revised
285 the manuscript critically and approved the article's final version for publication. MWP and CB supervised the study.

286 **Acknowledgements**

287 We thank all technical assistants who supported laboratory tasks.

288

289 References

- 290 ¹ Harbarth, S. *et al.* Universal screening for methicillin-resistant staphylococcus aureus at hospital admission and
291 nosocomial infection in surgical patients. *JAMA* **299**, 1149–1157 (2008).
- 292 ² Xu, L., Sun, X. & Ma, X. Systematic review and meta-analysis of mortality of patients infected with carbapenem-
293 resistant klebsiella pneumoniae. *Ann. Clin. Microbiol. Antimicrob.* **16**, 18 (2017).
- 294 ³ Armstrong, G. L. *et al.* Pathogen genomics in public health. *N. Engl. J. Med.* **381**, 2569–2580 (2019).
- 295 ⁴ Jousset, A. B. *et al.* A 4.5-year Within-Patient evolution of a Colistin-Resistant klebsiella pneumoniae Carbapenemase-
296 Producing k. pneumoniae sequence type 258. *Clin. Infect. Dis.* **67**, 1388–1394 (2018).
- 297 ⁵ Hall, J. P. J., Wood, A. J., Harrison, E. & Brockhurst, M. A. Source-sink plasmid transfer dynamics maintain gene
298 mobility in soil bacterial communities. *Proc. Natl. Acad. Sci. U. S. A.* **113**, 8260–8265 (2016).
- 299 ⁶ León-Sampedro, R. *et al.* Pervasive transmission of a carbapenem resistance plasmid in the gut microbiota of
300 hospitalized patients. *Nat Microbiol* **6**, 606–616 (2021).
- 301 ⁷ Carr, V. R. & Chaguza, C. Metagenomics for surveillance of respiratory pathogens. *Nat. Rev. Microbiol.* **19**, 285
302 (2021).
- 303 ⁸ de Siqueira, G. M. V., Pereira-dos Santos, F. M., Silva-Rocha, R. & Guazzaroni, M.-E. Nanopore sequencing provides
304 rapid and reliable insight into microbial profiles of intensive care units. *Frontiers in Public Health* **9**, 1231 (2021).
- 305 ⁹ He, Y. *et al.* Antibiotic resistance genes from livestock waste: occurrence, dissemination, and treatment. *npj Clean*
306 *Water* **3**, 1–11 (2020).
- 307 ¹⁰ Loose, M., Malla, S. & Stout, M. Real-time selective sequencing using nanopore technology. *Nat. Methods* **13**,
308 751–754 (2016).
- 309 ¹¹ Kovaka, S., Fan, Y., Ni, B., Timp, W. & Schatz, M. C. Targeted nanopore sequencing by real-time mapping of raw
310 electrical signal with UNCALLED. *Nat. Biotechnol.* **39**, 431–441 (2021).
- 311 ¹² Payne, A. *et al.* Readfish enables targeted nanopore sequencing of gigabase-sized genomes. *Nat. Biotechnol.* **39**,
312 442–450 (2020).
- 313 ¹³ Kipp, E. J. *et al.* Enabling metagenomic surveillance for bacterial tick-borne pathogens using nanopore sequencing
314 with adaptive sampling (2021).
- 315 ¹⁴ Koren, S., Phillippy, A. M., Simpson, J. T., Loman, N. J. & Loose, M. Reply to 'errors in long-read assemblies can
316 critically affect protein prediction'. *Nat. Biotechnol.* **37**, 127–128 (2019).
- 317 ¹⁵ Jia, B. *et al.* CARD 2017: expansion and model-centric curation of the comprehensive antibiotic resistance database.
318 *Nucleic Acids Res.* **45**, D566–D573 (2017).
- 319 ¹⁶ Steinegger, M. & Söding, J. MMseqs2 enables sensitive protein sequence searching for the analysis of massive data
320 sets. *Nat. Biotechnol.* **35**, 1026–1028 (2017).
- 321 ¹⁷ Kolmogorov, M., Yuan, J., Lin, Y. & Pevzner, P. A. Assembly of long, error-prone reads using repeat graphs. *Nat.*
322 *Biotechnol.* **37**, 540–546 (2019).

- 323 ¹⁸ Vaser, R., Sović, I., Nagarajan, N. & Šikić, M. Fast and accurate de novo genome assembly from long uncorrected
324 reads. *Genome Res.* **27**, 737–746 (2017).
- 325 ¹⁹ Li, H. Minimap2: pairwise alignment for nucleotide sequences. *Bioinformatics* **34**, 3094–3100 (2018).
- 326 ²⁰ Parks, D. H., Imelfort, M., Skennerton, C. T., Hugenholtz, P. & Tyson, G. W. CheckM: assessing the quality of
327 microbial genomes recovered from isolates, single cells, and metagenomes. *Genome Res.* **25**, 1043–1055 (2015).
- 328 ²¹ Chaumeil, P.-A., Mussig, A. J., Hugenholtz, P. & Parks, D. H. GTDB-Tk: a toolkit to classify genomes with the
329 genome taxonomy database. *Bioinformatics* **36**, 1925–1927 (2019).
- 330 ²² Pierce, N. T., Irber, L., Reiter, T., Brooks, P. & Brown, C. T. Large-scale sequence comparisons with *sourmash*.
331 *F1000Res.* **8**, 1006 (2019).
- 332 ²³ Van Damme, R. *et al.* Metagenomics workflow for hybrid assembly, differential coverage binning, metatranscrip-
333 tomics and pathway analysis (MUFFIN). *PLoS Comput. Biol.* **17**, e1008716 (2021).
- 334 ²⁴ Marçais, G. *et al.* MUMmer4: A fast and versatile genome alignment system. *PLoS Comput. Biol.* **14**, e1005944
335 (2018).
- 336 ²⁵ Bürkner, P.-C. Brms: An R package for bayesian multilevel models using stan. *J. Stat. Softw.* **80** (2017).
- 337 ²⁶ Nurk, S. *et al.* The complete sequence of a human genome (2021).